Atropisomerization of di-*para*-substituted propyl-bridged biphenyl cyclophanes

Jürgen Rotzler[†a], *Heiko Gsellinger*[†a], *Angela Bihlmeier*[†b,c], *Markus Gantenbein*[a], *David Vonlanthen*[a], *Daniel Häussinger**[a], *Wim Klopper**[b,c,d], *Marcel Mayor**[a,c,d]

[†] All authors contributed equally to this publication.

[a]Department of Chemistry, University of Basel, St. Johannsring 19, 4056 Basel, Switzerland

[b]Institute of Physical Chemistry, Karlsruhe Institute of Technology (KIT), Fritz-Haber-Weg 2, 76131 Karlsruhe, Germany

[c]Center for Functional Nanostructures (CFN), Karlsruhe Institute of Technology (KIT), Wolfgang-Gaede-Str. 1a, 76131 Karlsruhe, Germany

[d]Institute of Nanotechnology, Karlsruhe Institute of Technology (KIT), P. O. Box 3640, 76021 Karlsruhe, Germany

Supporting Information

Contents:

Synthesis of 1a, 1l, 1g and 1h

3,9-Dinitro-6,7-dihydro-5H-dibenzo[*a*,*c*][7]annulene (1a): Diamine **1k** (133 mg, 0.590 mmol, 1.00 equiv.) and KI (4.97 mg, 30.0 µmol, 5 mol%) were dissolved in 2 mL acetonitrile. To this solution 70% aq. TBHP (0.620 ml, 4.50 mmol, 7.60 equiv.) was added dropwise at 0°C. The black solution was stirred at 80°C overnight. After cooling the reaction mixture to rt, it was quenched with $Na_2S_2O_3$, washed with brine, extracted with ethyl acetate (3 x 20 mL) and dried with $MgSO_4$. The solvent was removed *in vacuo* and the residual crude was purified by column chromatography (SiO_2; cylohexane:CH_2Cl_2; 5:1, 1% MeOH) yielding **1a** as a white solid (31.5%).

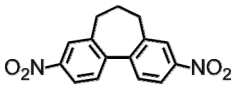

R_f = 0.71 (SiO_2; cyclohexane:CH_2Cl_2; 5:1, 1% MeOH); ^{1}H-NMR (400 MHz, $CDCl_3$): δ = 8.25 (dd, ^3J(H,H) = 8.4 Hz, ^4J(H,H) = 2.3 Hz, 2H, Ar-H), 8.18 (d, ^4J(H,H) = 2.3 Hz, 2H, Ar-H), 7.57 (d, ^3J(H,H) = 8.4 Hz, 2H, Ar-H), 2.62 (br. s, 4H), 2.32 (q, ^3J(H,H) = 7.0 Hz, 2H) ppm; ^{13}C-NMR (400 MHz, $CDCl_3$): δ = 148.1 (C_q, 2C), 145.6 (C_q, 2C), 141.3 (C_q, 2C), 129.5 (C_t, 2C), 123.9 (C_t, 2C), 122.3 (C_t, 2C), 32.7 (C_s, 2C), 31.2 (C_s, 1C); MS (EI +, 70 eV): m/z (%) = 284 (100), 267 (3), 237 (9), 191 (32), 165 (16), 152 (8); elemental analysis calcd (%) for $C_{15}H_{12}N_2O_4$: C 63.38, H 4.25, N 9.85; found: C 63.94, H 4.64, N 9.76.

3,9-Di(piperidin-1-yl)-6,7-dihydro-5H-dibenzo[*a*,*c*][7]annulene (1l): Diamine **1k** (177 mg, 0.789 mmol, 1.00 equiv.) was suspended in 3 mL water. To this suspension was added SDS (4.55 mg, 20.0 µmol, 2 mol%), $NaHCO_3$ (292 mg, 3.47 mmol, 4.40 equiv.) and 1,5-dibromopentane (798 mg, 3.47 mmol, 4.40 equiv.). The reaction mixture was then heated at 80°C for 2 h. After cooling to room temperature, 1 m NaOH was added to the mixture and extracted with 3 x 50 mL dichloromethane. The combined organic layers were dried with $MgSO_4$ and filtered. The solvent was removed under reduced pressure. Purification by column chromatography (SiO_2; cyclohexane:EtOAc; 3:1, 5% NEt_3) yielded **1l** as white solid (52%). For further analysis the product was recrystallized from pure ethyl acetate.

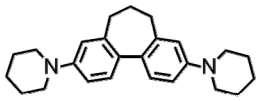

R_f = 0.89 (SiO_2; cyclohexane:ethyl acetate; 3:1, 5% NEt_3); ^{1}H-NMR (400 MHz, $CDCl_3$): δ = 7.22 (d, ^3J(H,H) = 8.3 Hz, 2H, Ar-H), 6.87 (dd, ^3J(H,H) = 8.3 Hz, ^4J(H,H) = 2.5 Hz, 2H, Ar-H), 6.82 (d,

^4J(H,H) = 2.5 Hz, 2H, Ar-H), 3.20-3.18 (m, 8H), 2.46 (t, ^3J(H,H) = 7.0 Hz, 4H), 2.14 (q, ^3J(H,H) = 7.0 Hz, 2H), 1.76-1.70 (m, 8H), 1.61-1.56 (m, 4H); ^{13}C-NMR (101 MHz, $CDCl_3$): δ = 151.1 (C_q, 2C), 140.2 (C_q, 2C), 132.3 (C_q, 2C), 128.5 (C_t, 2C), 116.7 (C_t, 2C), 114.24 (C_t, 2C), 50.8 (C_s, 2C), 33.1 (C_s, 2C), 32.2 (C_s, 1C), 26.0 (C_s, 2C), 24.4 (C_s, 2C); MS (ESI, positive ion mode, MeCN): m/z = 360 ([M^+]), 303, 180; elemental analysis calcd (%) for $C_{25}H_{32}N_2$: C 83.28, H 8.95, N 7.77; found: C 83.37, H 9.24, N 7.71.

3,9-Difluoro-6,7-dihydro-5H-dibenzo[*a*,*c*][7]annulene (1g):[1] To a suspension of diamine **1k** (110 mg, 1.00 equiv., 0.490 mmol) in 20 mL 48% tetrafluoroboric acid sodium nitrite (71.0 mg, 2.10 equiv., 1.03 mmol) dissolved in 4 mL H_2O was added dropwise at 0°C. 20 mL dichloromethane was added to completely dissolve the starting materials. After stirring at 0°C for 10 min the brown reaction mixture was irradiated with a mercury vapor lamp at 0°C overnight. Then 40% aqueous NaOH was added at 0°C for neutralization. The mixture was extracted three times with ethyl acetate. The combined organic layers where washed once with brine and dried with $MgSO_4$. After evaporation of the solvent, the crude was purified by column chromatography (SiO_2; cyclohexane) to achieve 100 mg (88%) of **1g** as a white solid. For further analysis difluoride **1g** was recrystallized from a mixture of methanol and water (25:1).

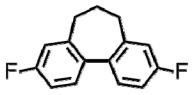

R_f = 0.49 (SiO_2; cyclohexane); ^{1}H-NMR (400 MHz, $CDCl_3$): δ = 7.28 (dd, ^3J(H,H) = 8.4 Hz, ^4J(H,F) = 5.7 Hz, 2H, Ar-H), 7.01 (td, ^3J(H,H) = 8.4 Hz, ^3J(H,F) = 2.7 Hz, 2H, Ar-H), 6.95 (dd, ^3J(H,H) = 9.3 Hz, ^3J(H,F) = 2.7 Hz, 2H, Ar-H), 2.46 (t, ^3J(H,H) = 7.1 Hz, 4H), 2.17 (q, ^3J(H,H) = 7.1 Hz, 2H) ppm; ^{13}C-NMR (101 MHz, $CDCl_3$): δ = 162.3 (d, ^1J(C,F) = 245.9 Hz, C_q, 2C), 141.7 (d, ^3J(C,F) = 7.4 Hz, C_q, 2C), 136.2 (d, ^4J(C,F) = 3.1 Hz, C_q, 2C), 129.8 (d, ^3J(C,F) = 8.3 Hz, C_t, 2C), 115.4 (d, ^2J(C,F) = 21.1 Hz, C_t, 2C), 113.4 (d, ^2J(C,F) = 21.2 Hz, C_t, 2C), 32.9 (C_s, 2C), 31.5 (C_s, 1C) ppm; MS (EI +, 70 eV): m/z (%) = 230.1 (100), 215.1 (41), 201.0 (24), 195.1 (12), 183.1 (6); elemental analysis calcd (%) for $C_{15}H_{12}F_2$: C 78.24, H 5.25; found: C 77.86, H 5.57.

6,7-Dihydro-5H-dibenzo[*a*,*c*][7]annulene (1h): The dibromide **1e** (50.0 mg, 1.00 equiv., 0.142 mmol) was dissolved in 2 mL THF (abs., crown-cap) under argon

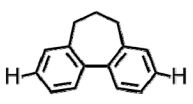

atmosphere and cooled to −78°C. Then *t*-BuLi (0.373 mL, 246 mg, 4.20 equiv., 0.596 mmol) was added dropwise. The reaction mixture (green) was stirred at the elevated temperature for 1.5 h. Then 2 mL sat. aq. ammonium chloride solution was added and after stirring for 30 min at rt the phases were separated. The aqueous one was extracted twice with cyclohexane. The combined organic layers were washed with brine, dried with sodium sulfate, filtered and concentrated. The crude was purified by column chromatography (SiO_2; cyclohexane). According to the described procedure the desired target compound was obtained as a colorless liquid.

R_f = 0.41 (SiO_2; cyclohexane); ^{1}H-NMR (400 MHz, $CDCl_3$): δ = 7.39 (dd, ^3J(H,H) = 7.2 Hz, ^4J(H,H) = 1.6 Hz, 2H, Ar-H), 7.35 (dt, ^3J(H,H) = 7.2 Hz, ^4J(H,H) = 1.6 Hz, 2H, Ar-H), 7.30 (dt, ^3J(H,H) = 7.2 Hz, ^4J(H,H) = 1.6 Hz, 2H, Ar-H), 7.25 (dd, ^3J(H,H) = 7.2 Hz, ^4J(H,H) = 1.6 Hz, 2H, Ar-H), 2.51 (t, ^3J(H,H) = 7.1 Hz, 4H), 2.20 (quint, ^3J(H,H) = 7.1 Hz, 2H) ppm. The analytic data is according to literature.[2]

NMR temperature calibration

Temperature calibration is needed for variable temperature NMR spectroscopy as the temperature unit is placed below the sample and therefore gives only a hint of the stability and absolute value of the temperature. For temperature calibration a CH_3OH (4 %) in CD_3OD (96 %) sample was used. The temperature calibration was performed using equation (1) for temperatures between 200 – 265 K and equation (2) for temperatures between 265 – 300 K.

$$T = (3.92 - \Delta\delta) / 0.008 \qquad (1)$$

$$T = (4.109 - \Delta\delta) / 0.008708 \qquad (2)$$

T = absolute temperature [K], $\Delta\delta$ = chemical shift difference between CH_3 and OH resonance in MeOH [ppm].[3]

Each temperature was measured three times to prove the stability of the system. The temperature variation during the experiment is less than 0.05 K and therefore much smaller than the estimated calibration error of 1 K. In Figure S1 the calibration curve with its statistical errors is depicted. All temperatures used for the calculation of thermodynamic data were normalized to the calibrated temperature data.

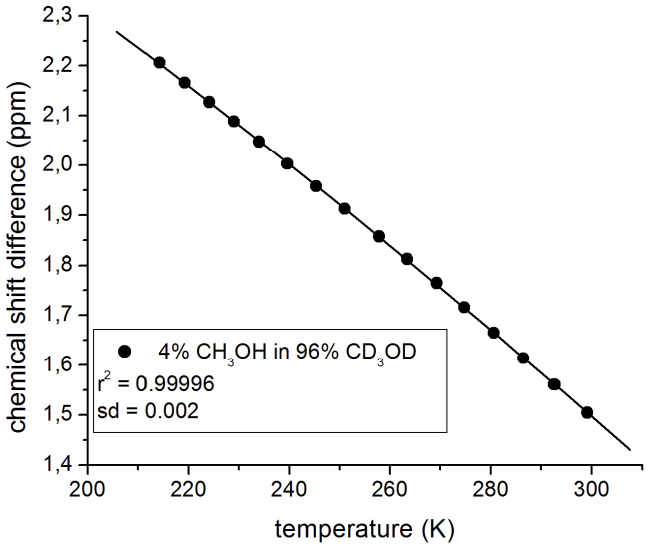

Figure S1: Temperature calibration for low temperature NMR experiments with a CH_3OH (4 %) in CD_3OD (96 %) sample.

Variable temperature NMR spectra

All samples were prepared in deuterated solvents (> 99.8 % D, Cambridge Isotope Laboratories, Burgdorf, CH). The NMR experiments were performed on a Bruker Avance III – 600 MHz NMR spectrometer, equipped with a self-shielded z-axis pulsed field gradient dual channel broadband inverse probe-head. For thermodynamic investigations three different states have to be accessible. The *slow exchange* where the signals of the two protons are obtained as well separated resonances, the *coalescence* where the signal reaches a plateau and the line width is extremely broadened, and finally the *fast exchange* where the signals are obtained as an averaged signal.

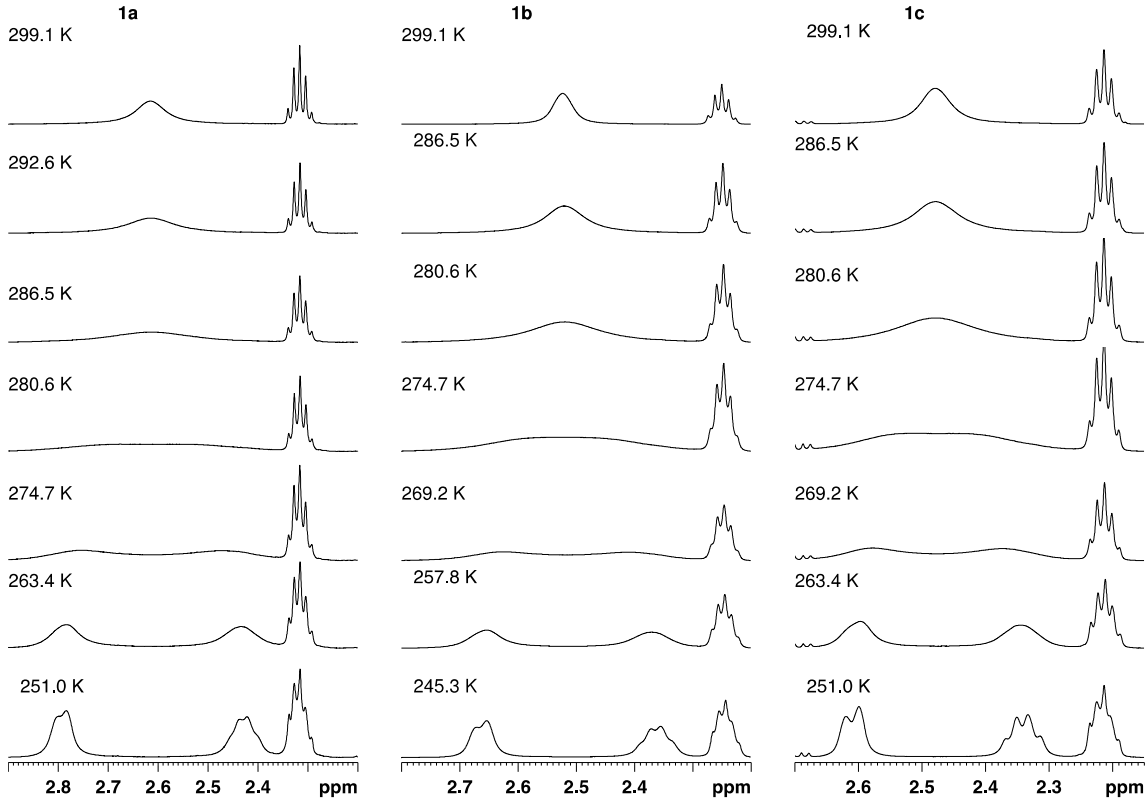

Figure S2: Experimental NMR spectra of **1a**, **1b** and **1c** at variable temperatures.

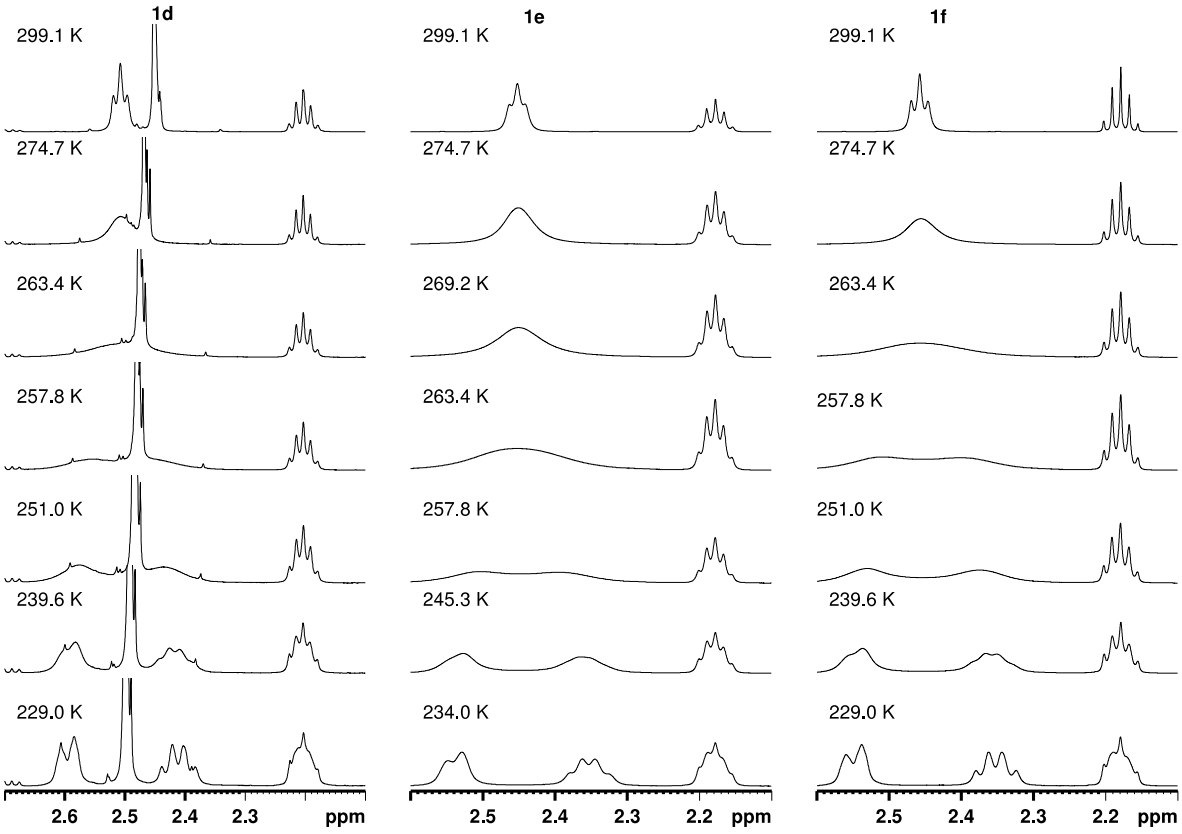

Figure S3: Experimental NMR spectra of **1d**, **1e** and **1f** at variable temperatures.

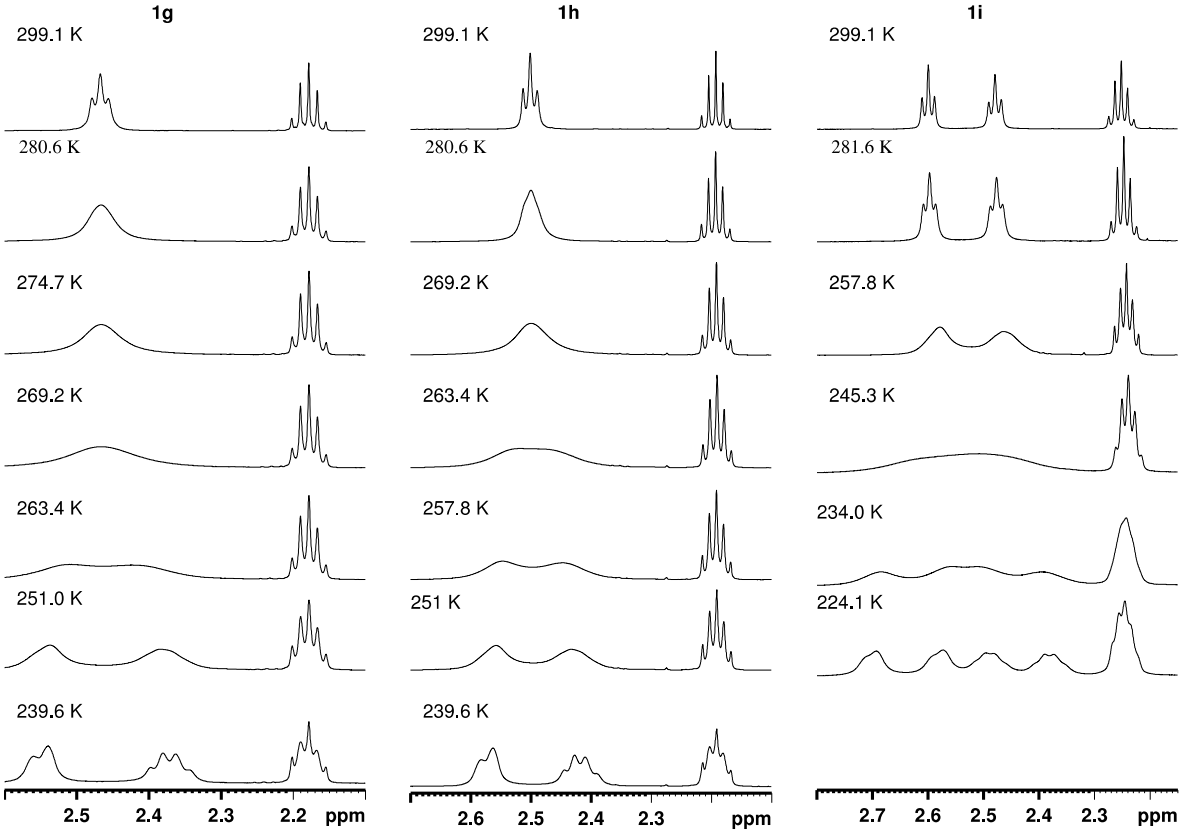

Figure S4: Experimental NMR spectra of **1g**, **1h** and **1i** at variable temperatures.

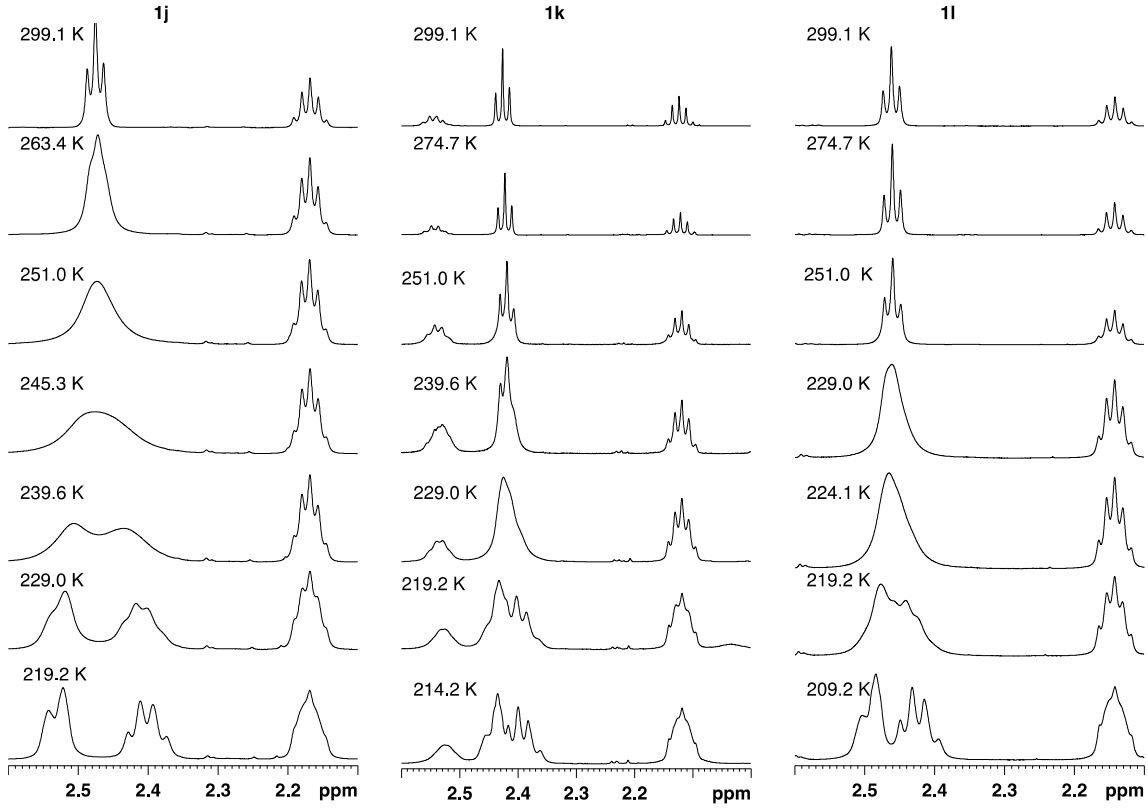

Figure S5: Experimental NMR spectra of **1j**, **1k** and **1l** at variable temperatures.

Calculation of coalescence temperatures $T_{c\text{-lineshape}}$

The coalescence temperatures were calculated from the line width of the coalescent peak. The line width was therefore plotted against the temperature and the resulting points were fitted with a Lorentzian shaped curve. A good agreement with the experimental coalescence temperatures T_c was obtained except for the dipiperidinyl substituted biphenyl **1l**. Limiting factor was the freezing point of $CDCl_3$. An example for the determination of the coalescence temperature is shown in figure S6. The maximum of the calculated curve delivers directly the coalescence temperature.

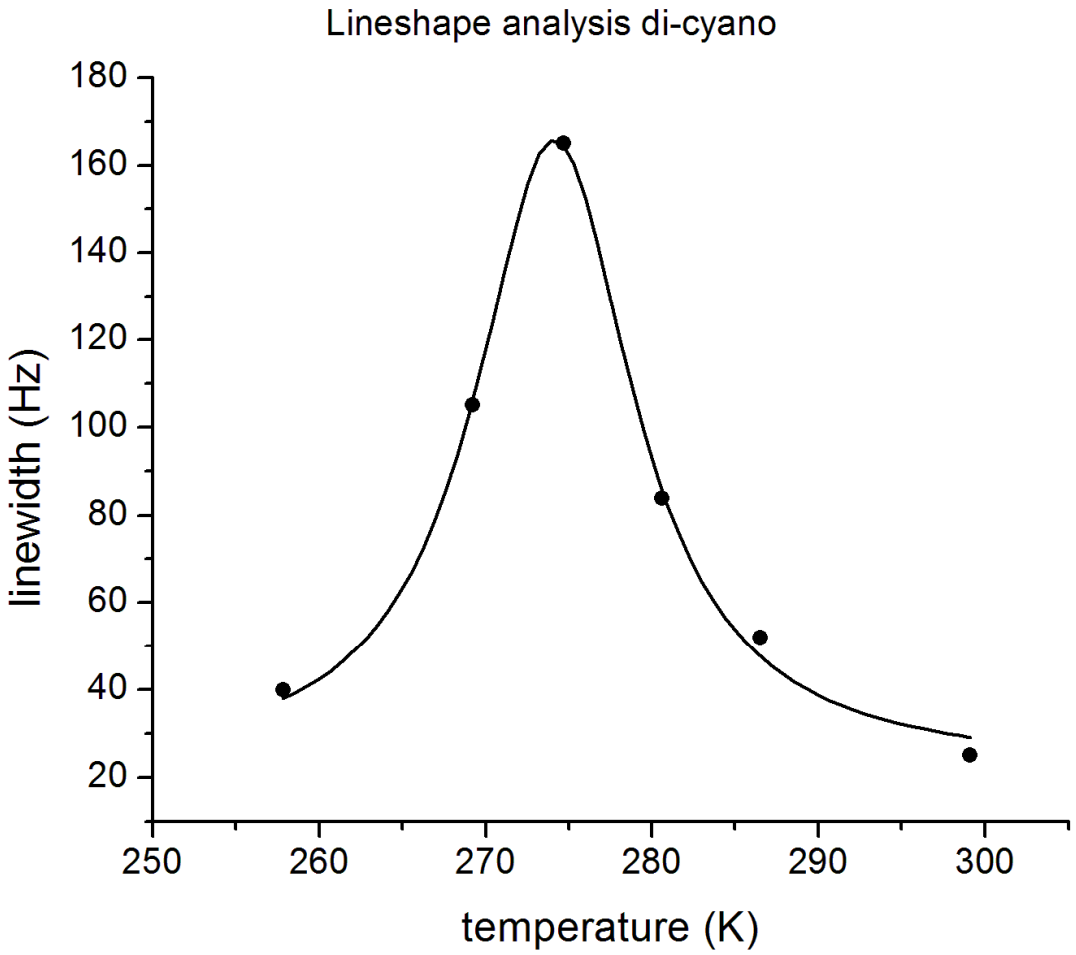

Figure S6: Calculation of the coalescence temperature from the line width of the coalescent peak.

Rate constants

Experimental rate constants were obtained from lineshape analysis.

1a	*fitted*	**1b**	*fitted*	**1c**	*fitted*
T	*k*	*T*	*k*	*T*	*k*
299.1	2000	299.1	3050	299.1	3800
292.6	1200	286.5	1200	286.5	1450
286.5	760	280.6	705	280.6	900
280.6	450	274.7	415	274.7	560
274.7	290	269.2	260	269.2	340
263.4	97	257.8	90	263.4	200
251.0	35			251.0	65
				239.6	21

1d	*fitted*	**1e**	*fitted*	**1f**	*fitted*
T	*k*	*T*	*k*	*T*	*k*
299.1	4200	274.7	850	299.1	4800
286.5	1900	269.2	515	286.6	2050
274.7	820	263.4	295	274.7	810
269.2	500	257.8	172	269.2	500
263.4	320	245.3	55	263.4	325
257.8	180			257.8	185
251.0	105			251.0	105
239.6	35			239.6	38
				229.0	13

1g	*fitted*	**1h**	*fitted*	**1i**	*fitted*
T	*k*	*T*	*k*	*T*	*k*
299.1	3100	299.1	3200	299.1	10200
280.6	840	280.6	1000	281.6	4200
274.7	530	269.2	395	257.8	820
269.2	315	263.4	195	245.3	345
263.4	186	257.8	128	234.0	130
251.0	63	251.0	72	224.1	50
239.6	22	239.6	25		

1j	*fitted*	**1k**	*fitted*	**1l**	*fitted*
T	*k*	*T*	*k*	*T*	*k*
274.7	1500	251.0	550	274.7	1500
263.4	950	239.6	230	263.4	900
251.0	380	234.0	160	251.0	600
245.3	180	229.0	100	239.6	400
239.6	104	224.0	50	229.0	175
229.0	37	219.2	32	224.1	120
219.2	16	214.2	20	219.2	54
				209.2	21

Overview of Eyring plots

All experimental NMR spectra were fitted to obtain rate constants for the rotation process. These rate constants were then further analyzed with Eyring plots ($R^2 \geq 0.99$, except for Pip) to get deeper insight into thermodynamic data.

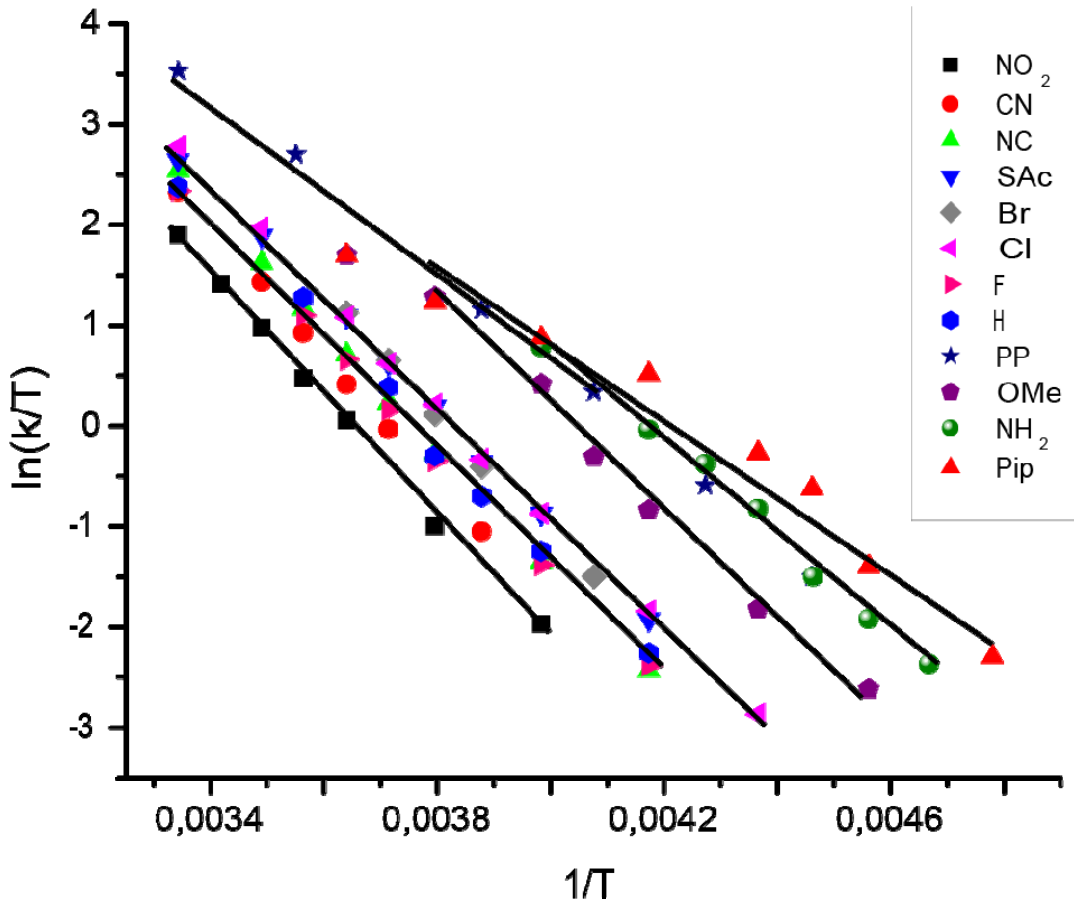

Figure S7: Eyring plots of the investigated propyl-bridged biphenyls **1a** – **1l**.

Determination of the Standard Deviation for $\Delta H_{\mathrm{Eyring}}^{\ddagger}$, $\Delta S_{\mathrm{Eyring}}^{\ddagger}$, $\Delta G_{\mathrm{Eyring}}^{\ddagger}$

The standard deviations σ for the enthalpy, entropy, and Gibbs free energy values given in Table 2 of the main paper were obtained from the following procedure: firstly, the experimental reaction rate constants $\ln(k/T)$ were plotted against $1/T$ in a single Eyring plot and fitted by linear regression. From this fit, the values $\Delta H_{\mathrm{Eyring}}^{\ddagger}$, $\Delta S_{\mathrm{Eyring}}^{\ddagger}$, and $\Delta G_{\mathrm{Eyring}}^{\ddagger}$ given in Table 2 of the main paper were obtained. Secondly, at the experimental temperatures T_i, $i = 1, \ldots, n$, the corresponding reaction rate constants k_i were computed from the equation

$$k_i = k_{\mathrm{B}} T_i \exp\{-(\Delta H_{\mathrm{Eyring}}^{\ddagger} - T_i \Delta S_{\mathrm{Eyring}}^{\ddagger})/(RT_i)\} / h\,, \quad i = 1, \ldots, n\,.$$

Obviously, these computed points lie on a perfect straight line. Thirdly, a total number of $j = 1, \ldots, 2500$ individual simulations were performed. In each of these simulations, n data points $(T_i+\delta_T, k_i+\delta_k)$ were generated using a random number generator, taking random numbers δ_T and δ_k from a Gaussian distribution about the temperature T_i and about the reaction rate constant k_i. The Gaussian distributions were chosen according to the standard deviations of $\sigma_T = 1$ K and $\sigma_k = 5\%$, respectively. An Eyring plot for these n data points yielded $\Delta H_{\mathrm{Eyring}}^{\ddagger}(j)$, $\Delta S_{\mathrm{Eyring}}^{\ddagger}(j)$, and $\Delta G_{\mathrm{Eyring}}^{\ddagger}(j)$. Finally, the standard deviations σ for the enthalpy, entropy, and Gibbs free energy values given in Table 2 were obtained from the distribution of the 2500 values obtained in the simulations. As an illustration, Figure S8 shows all of the 2500 data points used in the above procedure for **1b**, which involved $2 \times 6 \times 2500 = 30000$ random numbers in total.

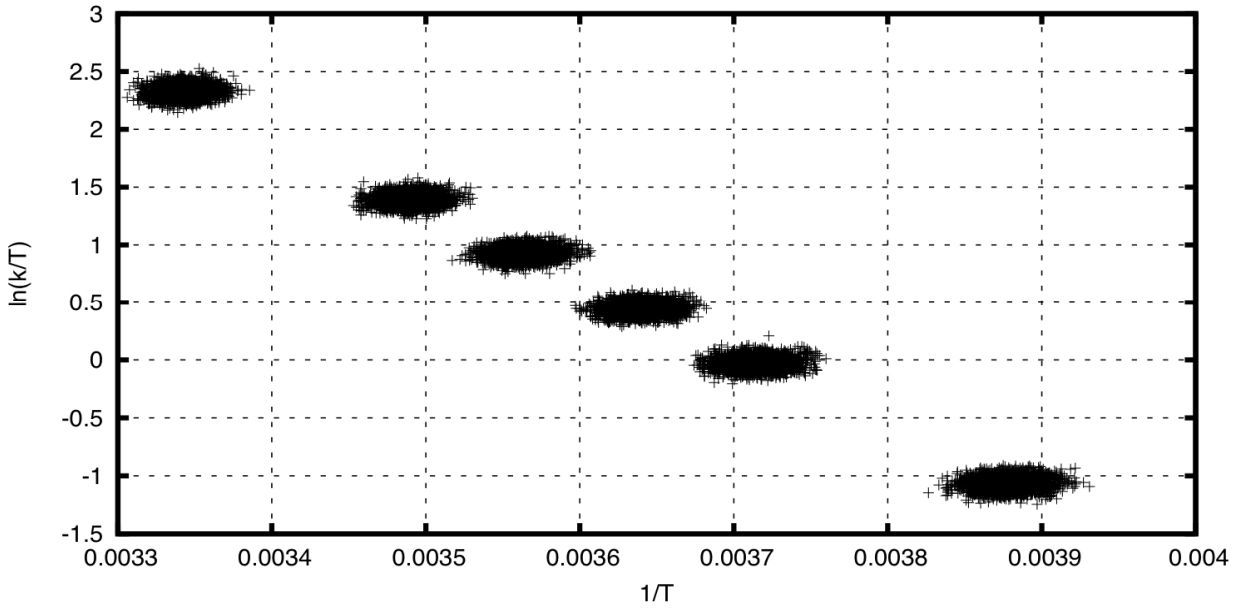

Figure S8. Data points for **1b** from 2500 simulations (n = 6).

Hammett correlations of $\Delta H_{Eyring}^{\ddagger}$ and $\Delta S_{Eyring}^{\ddagger}$

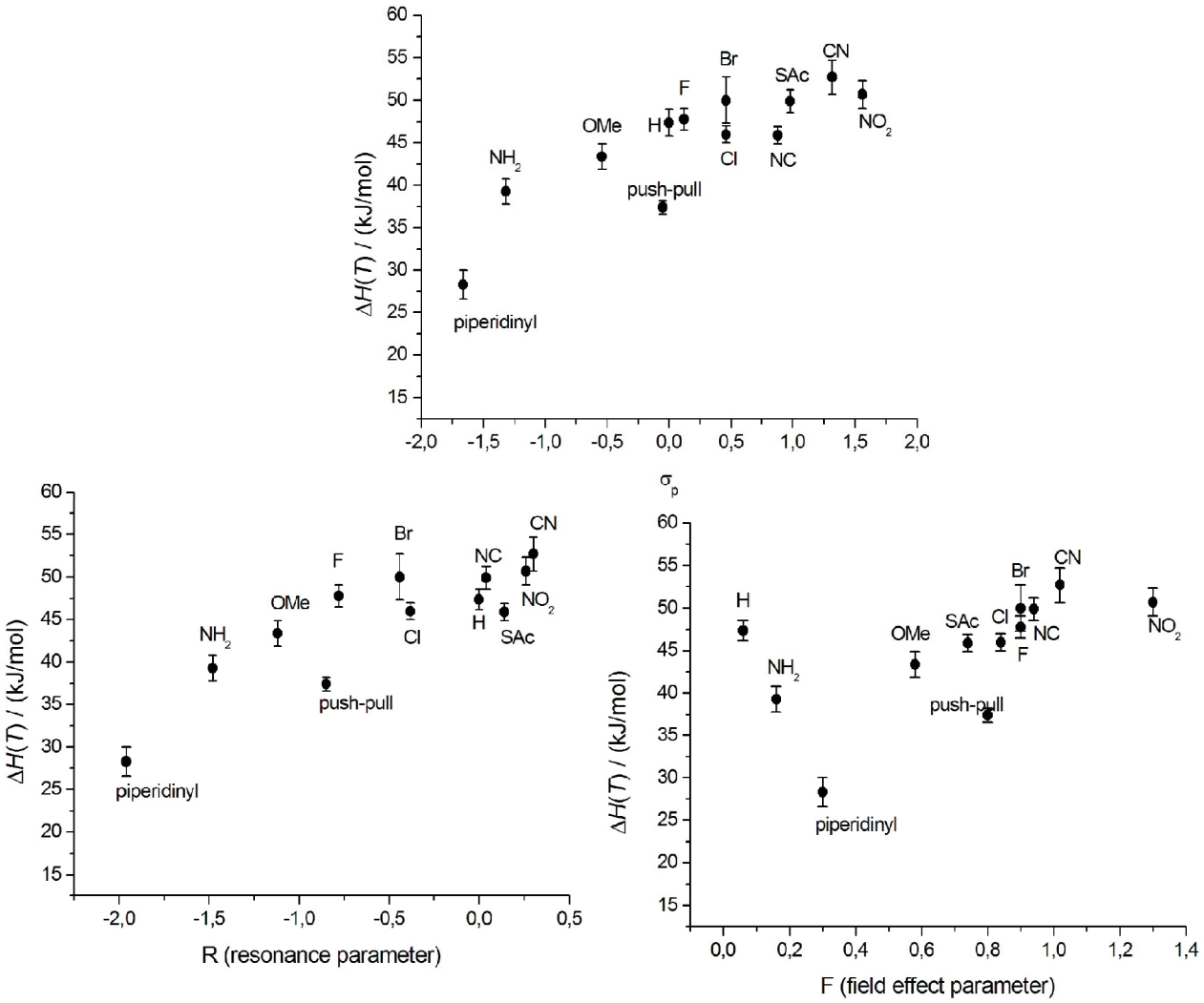

Figure S9. Correlation of the entropies $\Delta H_{Eyring}^{\ddagger}$ with the Hammett-parameter σ_p (top), the resonance parameter R (bottom left), and the field effect parameter F (bottom right).

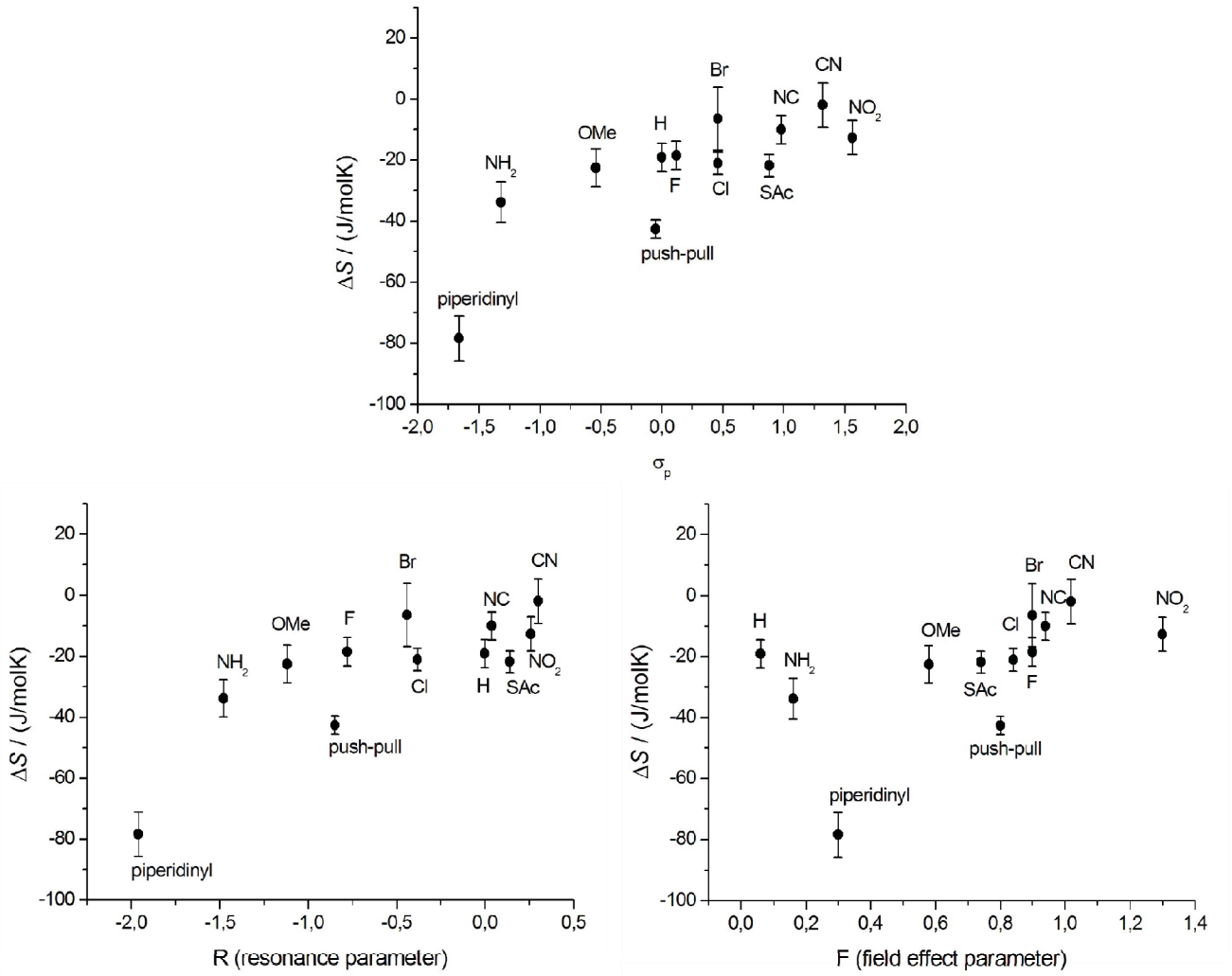

Figure S10. Correlation of the entropies $\Delta S_{Eyring}^{\ddagger}$ with the Hammett-parameter σ_p (top), the resonance parameter R (bottom left), and the field effect parameter F (bottom right).

Solvent influence on NMR spectra

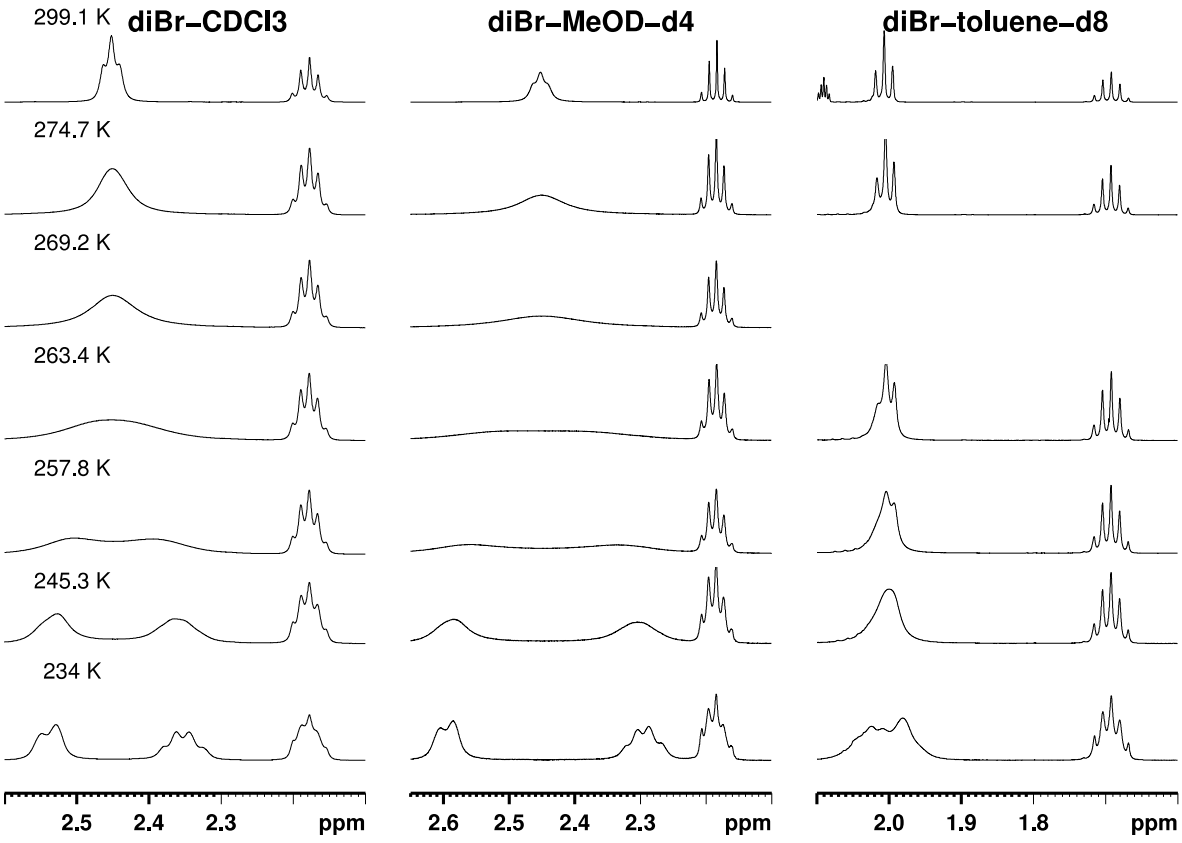

Figure S11. Solvent dependent NMR spectra of **1e** at variable temperatures.

The solvent dependent NMR spectra showed different coalescence temperatures (T_c) and different shift differences (Δν). $\Delta G^{\ddagger}(T)$ is dependent on both as shown in eqn (3).[4] Our investigations show that $\Delta G^{\ddagger}(T)$ remains constant for all investigated solvents. The solvent effect on the thermodynamic data obtained by line shape analyses of ^{1}H-NMR coalescence measurements in different solvents is summarized in the following table.

	1e ($CDCl_3$)	**1e** (MeOD)	**1e** (toluene)
$\Delta S_{Eyring}^{\ddagger}$ / J/(mol K)	−6.4 ± 10.4	−8.0 ± 4.6	−18.0 ± 5.5
$\Delta H_{Eyring}^{\ddagger}$ / kJ/mol	50.0 ± 2.7	49.0 ± 1.3	45.9 ± 1.4
$\Delta G_{Eyring}^{\ddagger}$ / kJ/mol	51.7 ± 0.1	51.1 ± 0.1	50.4 ± 0.1
$\Delta G^{\ddagger}$ / kJ/mol	51.3 ± 0.5	51.0 ± 0.5	50.5 ± 0.5
	1b ($CDCl_3$)	**1b** (MeOD)	**1b** (toluene)

$\Delta S_{Eyring}^{\ddagger}$ / J/(mol K)	−1.9 ± 7.3	−8.3 ± 4.2	−39.9 ± 3.5
$\Delta H_{Eyring}^{\ddagger}$ / kJ/mol	52.7 ± 2.0	50.1 ± 1.2	41.7 ± 0.9
$\Delta G_{Eyring}^{\ddagger}$ / kJ/mol	53.2 ± 0.1	52.3 ± 0.1	51.9 ± 0.1
$\Delta G^{\ddagger}$ / kJ/mol	53.3 ± 0.5	52.4 ± 0.5	52.0 ± 0.5
	1j ($CDCl_3$)	**1j** (MeOD)	**1j** (toluene)
$\Delta S_{Eyring}^{\ddagger}$ / J/(mol K)	−22.5 ± 6.2	−12.8 ± 4.0	−5.0 ± 4.9
$\Delta H_{Eyring}^{\ddagger}$ / kJ/mol	43.4 ± 1.5	45.6 ± 1.0	47.9 ± 1.3
$\Delta G_{Eyring}^{\ddagger}$ / kJ/mol	48.8 ± 0.1	48.7 ± 0.1	49.1 ± 0.1
$\Delta G^{\ddagger}$ / kJ/mol	48.4 ± 0.5	48.5 ± 0.5	48.9 ± 0.5

In this study, methanol as a polar protic solvent and toluene as a π-donating solvent were chosen to gain insight into the stabilizing effect on the transition state. Therefore a donor-substituted (**1j**), a neutral (**1e**) and an acceptor-substituted biphenyl (**1b**) were measured in both solvents and then compared to the thermodynamic data obtained in chloroform. In all cases the free energy $\Delta G^{\ddagger}(T)$ remained similar in all solvents, whereas the enthalpies $\Delta H^{\ddagger}$ and the entropies $\Delta S^{\ddagger}$ significantly changed when measured in different solvents. It seems that the transition state of the atropisomerization process gets stabilized by protic solvents in the case of dimethoxy substituted propyl bridged biphenyls (**1j**). The opposite was observed for dicyano (**1b**) and dibromo (**1e**) substituted biphenyls where the transition state is most stabilized in toluene, a π-donating solvent. The reason for this remains unclear, especially because the entropy follows the opposite trend, and the free energy remains unchanged. It is hypothesized that a partial positive charge in the acceptor-substituted cases is stabilized by the electron rich toluene. Thus the energy needed to access the transition state in the atropisomerization process is lowered. On the contrary this solute-solvent complex results in a higher order in the ensemble in the transition state leading to negative entropies. The stabilization by protic solvents of the partial negative charge in donor substituted biphenyl **1j** would explain the opposed trend observed in this limited series of solvent depended coalescence

measurements. Nevertheless, the values obtained by lineshape analysis have to be regarded with caution due to the susceptibility of the Eyring analysis to errors in such a narrow temperature region.

(1) Dolensky, B. *J. Fluorine Chem.* **2001**, *107*, 147.
(2) Müllen, K.; Heinz, W.; Klärner, F.; Roth, W. R.; Kindermann, I.; Adamczak, O.; Wette, M.; Lex, J. *Chem. Ber.* **1990**, *123*, 2349–2371.
(3) Berger, S.; Braun, S. *200 and More NMR Experiments: A Practical Course*; 1. Aufl.; Wiley-VCH Verlag GmbH & Co. KGaA, 2004.
(4) Hesse, M.; Meier, H.; Zeeh, B. *Spektroskopische Methoden in der organischen Chemie*; 7., überarb. Aufl.; Thieme, Stuttgart, 2005.